Report

Ship-borne electromagnetic induction sounding of sea ice thickness in the Arctic during summer 2003

Kunio Shirasawa[1], Kazutaka Tateyama[2*], Toru Takatsuka[1]
Toshiyuki Kawamura[1] and Shotaro Uto[3]

[1]*Institute of Low Temperature Science, Hokkaido University,
Kita-19, Nishi-8, Kita-ku, Sapporo 060-0819*
[2]*Department of Civil Engineering, Kitami Institute of Technology,
165, Koen-cho, Kitami 090-8507*
[3]*National Maritime Research Institute, 6–38–1, Shinkawa, Mitaka-shi, Tokyo 181-0004*
[*]*Corresponding author. E-mail: tateyaka@mail.kitami-it.ac.jp*

Abstract: Measurements of ice thickness were carried out by a ship-borne electromagnetic induction instrument mounted on the R/V *Xuelong* during the Second Chinese National Arctic Research Expedition (CHINARE-2003) in summer 2003 in the Chukchi Sea. A 1-D multi-layer model, consisting of three layers of snow, ice and seawater, was used to calculate the total thickness of snow and sea ice. The time series of total thickness from 24 August to 7 September 2003 indicates that deformed and second-/multi-year ice floes appear frequently in very close pack ice farther from the ice edge, while thinner ice floes less than 1 m are frequently found in open pack ice. The probability density function of total thickness shows that a major peak appears at around 1.5 m thickness in very close pack ice, presumably corresponding to second-year or deformed ice. Also shown is a peak at around 0.3 m thickness, corresponding to typical level ice in open pack ice.

key words: Arctic, sea ice thickness, electro-magnetic inductive device (EM)

1. Introduction

The Arctic is recognized to be an important environment in the global climate system. Observational evidence of atmospheric and climate-sensitive variables such as sea ice, ocean water masses, river discharge, snow cover, glaciers and permafrost indicates that a reasonably coherent portrait of late 20th century change in the Arctic and sub-Arctic is apparent (*e.g.*, Bobylev *et al.*, 2003).

In the context of the International Arctic Science Committee (IASC)'s research priorities, the First and Second Chinese National Arctic Research Expeditions were organized in 1999 and 2003, respectively, to conduct a variety of scientific programs in the Bering Sea, the Chukchi Sea and the Canadian Basin of Arctic Ocean. One of the research programs was to understand the process of the Arctic sea ice change and its influence on the air/sea/sea ice exchange.
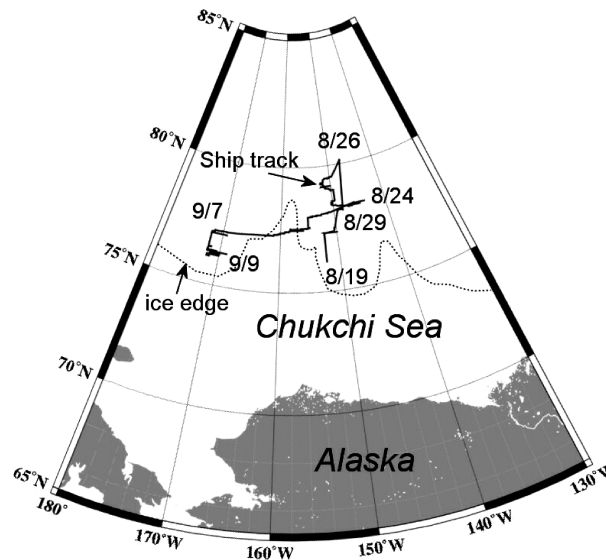
Fig. 1. The tracks of the R/V Xuelong (solid line) during the period from 19 August to 9 September 2003 in the Chukchi Sea. The dashed line shows the ice edge, derived from DMSP SSM/I data at the end of August 2003.

The objective of the present study was to measure the thickness of sea ice by the ship-borne electromagnetic induction instrument (hereafter denoted as SEM) mounted on the R/V *Xuelong* during the Second Chinese National Arctic Research Expedition (CHINARE-2003). SEM observations were conducted during the period from 19 August to 9 September 2003. Figure 1 indicates the tracks of the R/V *Xuelong* during SEM observations in the Chukchi Sea, together with the ice edge derived from DMSP SSM/I data at the end of August 2003.

2. Measurements

Combining an electromagnetic induction (EM) instrument with a laser altimeter is a widely used technique for measuring sea ice thickness from icebreakers (*e.g.*, Kovacs and Morey, 1991; Haas *et al.*, 1997; Worby *et al.*, 1999; Uto *et al.*, 2002). The ship-borne EM (SEM) utilized in the present study was a single frequency EM sensor (EM-31/ICE, Geonics Ltd., Canada), having two coils; a transmitter (Tx) and a receiver (Rx) at both ends. It can measure the distance from the sensor to the bottom of sea ice; namely the ice-water interface, in other words the surface of sea water. A laser altimeter (LD90-3100HS, Riegl Japan Ltd., Japan) detects the distance from the sensor to the top surface of snow or ice. Figure 2a is a schematic of ice thickness measurements by the SEM. The operating frequency is 9.8 kHz, and the distance between Tx and Rx is 3.66 m. The Tx generates an alternating primary magnetic field H_p and induces small eddy currents in the underlying seawater. These currents generate a secondary magnetic field H_s, which is sensed along with H_p by Rx. The EM instrument automatically transforms the measured quadrature response of H_s to the apparent conductivity σ_a in mS/m (McNeill, 1980). σ_a is defined as
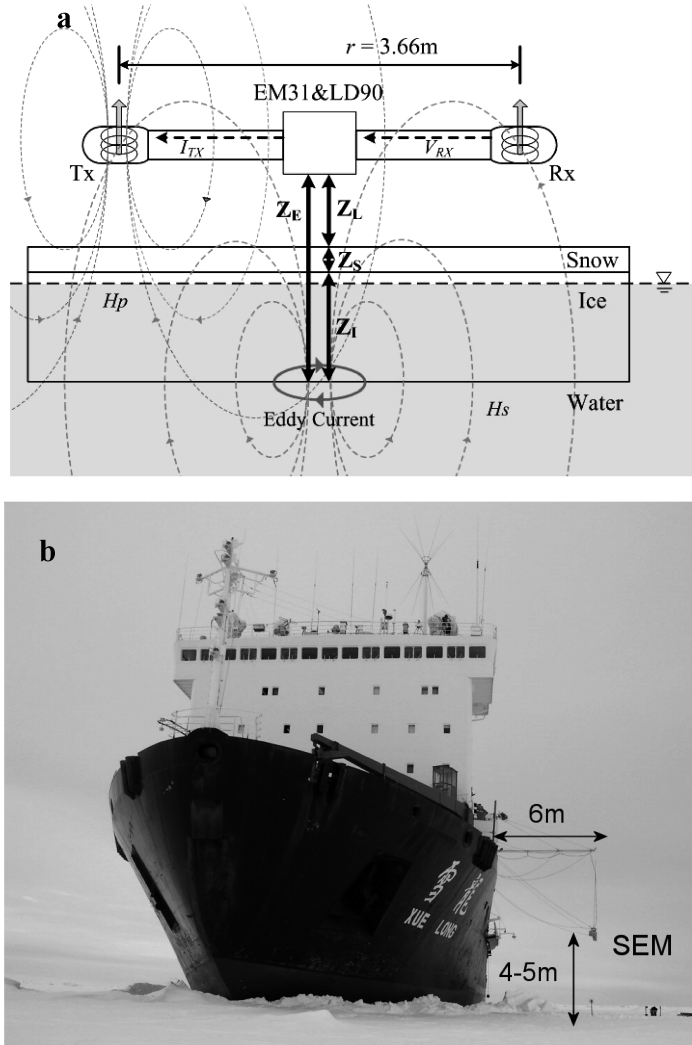
Fig. 2. *a) Principle of SEM measurement of total thickness of snow and sea ice. EM31 is an electromagnetic induction sensor, and LD90 is a laser distance sensor. Z_E, Z_L, Z_S, and Z_I are distances from the sensor to the ice bottom, the snow surface, the snow depth and the ice thickness, respectively. b) The ship-borne electromagnetic induction instrument (SEM) onboard the R/V Xuelong.*

$$\sigma_a = \frac{4}{\omega \mu_0 r^2} Q\left(\frac{H_s}{H_p}\right), \tag{1}$$

where μ_0, ω, r, and $Q(H_s/H_p)$ denote the magnetic permeability of free space ($4\pi \times 10^{-7}$ H/m), angular frequency ($\omega = 2\pi f$), transmitter-receiver coil separation (3.66 m) and the quadrature component of the ratio of H_s to H_p at Rx, respectively. The frequency (f) is 9.8 kHz.

Since the difference in conductivity between snow and ice is very small, the EM instrument cannot distinguish snow from ice. Therefore, we discuss the relationship between

σ_a derived from SEM measurements and the observed total thickness of snow and ice ($Z_S +$ Z_I, where Z_S is the snow depth and Z_I is the ice thickness). The total thickness can be calculated by subtracting the distance between the EM sensor and the snow/ice surface (Z_L) measured by a laser altimeter from the distance between the EM sensor and the seawater surface (Z_E).

σ_a can be measured in either the horizontal coplanar (HCP) mode or the vertical coplanar (VCP) mode of the EM instrument. In the present study we used the latter mode, since it has a finer lateral resolution than the HCP mode and possesses a high capability of distinguishing thin ice (Reid *et al.*, 2003). According to Reid and Vrbancich (2004), the footprint size for the VCP geometry is 1.4–1.5 times larger than Z_E; *i.e.* when sounding a 6-m-thick ice ridge at an instrument height of 4 m ($Z_E = 10$ m), the apparent footprint size for the VCP mode is 14–15 m. Therefore, the instrument should be placed 5.6–6.0 m away from the ship hull for the VCP mode at an operating height of 4 m (Fig. 2b), so that the effect of the ship hull can be prevented from affecting the observed data.

2.1. Calibration and core sampling

The output of the EM instrument was calibrated by measuring stepwise changes of sensor height over a 2.39-m-thick multi-year ice floe covered with a 0.26-m-deep snow layer on 29 August. The relation between the apparent conductivity (σ_a) and the distance between the EM instrument and the seawater surface (Z_E) is shown in Fig. 3a.

Snow, ice and seawater samples were collected from the site where the EM instrument was calibrated. The ice temperature was measured *in-situ* using a thermistor stick inserted into holes drilled at 5 or 10-cm intervals in the sample cores. These ice cores were cut into 5 to 10-cm sections and melted out on the ship. Sea-ice conductivity (σ_I) was measured from the melted ice water. The snow density and temperature were measured at 1–3 cm vertical intervals, and snow conductivity (σ_S) was measured from the melted samples. Ship-based CTD profile data were used for seawater conductivity (σ_W). Finally, the values of Z_S, Z_I, σ_S, σ_I, and σ_W were derived as 0.26 m, 2.39 m, 0 mS/m, 15 mS/m, 2270 mS/m, respectively. The conductivity values of ice and seawater obtained in the present study were smaller than those previously obtained in spring and summer in the Arctic and sub-Arctic (Tateyama *et al.*, 2006). In the present study, significant desalination might have occurred as the ice core samples were obtained from the second-/multi-year ice floes and less saline waters were found just below the ice prior to the onset of freezing.

2.2. Data reduction

A method to calculate $Z_S + Z_I$ from σ_a by using a 1-D multi-layer model was proposed by Haas *et al.* (1997) and Haas (1998). In the present study, we used a theoretical calculation program, PCLOOP developed by Geonics Ltd. (McNeill, 1980) to calculate σ_a using the 1-D multi-layer model, which consists of three layers, snow (Z_S, σ_{SBULK}), ice (Z_I, σ_{IBULK}) and seawater (infinite depth, σ_W). The instrument height (Z_L) was also included in this model.

The σ_a–Z_E transform equation is based on an empirical approximation of the analytical equation for the measured electromagnetic field. An approximation for the inversion model, which calculates Z_E from σ_a, is commonly used and gives stable results (Pfaffling *et al.*, 2004).
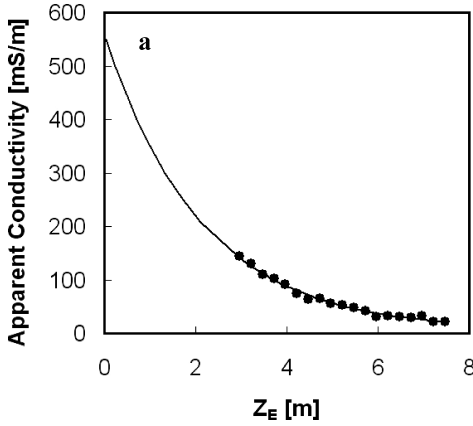
*Fig. 3a. The σ_a–Z_E relationship derived from chang-
ing the EM instrument height in the Chukchi
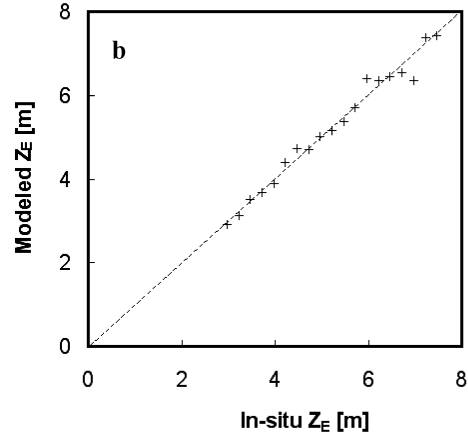Sea. The solid curve is an exponential fit.*

*Fig. 3b. The relationship between Z_E values obtained
from in-situ measurements and those calcu-
lated from eq. (2).*

$$Z_E = a_0 - \ln(\sigma_a - a_1)/a_2, \qquad (2)$$

where a_n are coefficients. The σ_a–Z_E relationship was derived from calibrations done by
varying the SEM instrument height over the 2.39-m-thick multi-year ice floe covered with a
0.26-m-deep snow layer, as shown in Fig. 3a. From the 1-D multi-layer model, a_0, a_1 and a_2
were derived as 13.47, 5.19 and 0.48, respectively.

The comparison between Z_E values measured *in-situ* and those estimated from eq. (2)
is shown in Fig. 3b. Estimated Z_E values agree well with the measured ones within 8%
error.

3. Results and discussion

SEM ice thickness data were obtained for 24–29 August and 4–7 September 2003.
First, the time series of σ_a records obtained at the sampling rate of 10 Hz were processed
with a 1001st low-pass digital filter, which cuts off the signal higher than 0.5 Hz, in order to
reduce the noise level from 0 db to –80 db. Those noises might be induced from the sig-
nal/power cable. After removing the noises, the total ice thickness was then calculated by
subtracting Z_L from Z_E estimated by eq. (2).

The time series of total thickness was combined with the time series of GPS (Global
Positioning System) position of the EM instrument obtained at the sampling interval of 0.5
Hz. The total thickness is shown as a function of time for 24–29 August and from 4–7
September, in Figs. 4 and 5, respectively. Thickness values were obtained every 2 s in Figs. 4
and 5 from time 0 (00h00m00s) to 43199 (23h59m58s). The hatched area shows no data.
SEM measurements during the first period in Fig. 4 were carried out in regions farther from
the ice edge (see Fig. 1), which were compact ice fields mainly filled with deformed and
second-/multi-year ice floes. In the beginning of the first period from 24 to 26 August in
Fig. 4, the ship proceeded northward, where approximately 0.3-m-thick ice, 1.5 to 2.0-m-

thick second-year ice and 4-m-thick multi-year ice were dominant. At the end of the first period from 27 to 29 August in Fig. 4, the ship headed towards the south through a rather loose ice area. After ramming into a thicker multi-year ice field, the ship anchored in large multi-year ice for establishing the ice station until 4 September. The probability density function (PDF) of total thickness in the 0.1 m bin size obtained from all data during the first period is shown in Fig. 6a. All ice over 6.1-m-thick was classified as 6.1-m-thick ice. The primary peak appeared at around 1.5 m, presumably corresponding to second-year ice; a peak at around 0.3 m was also found.

During the second period in Fig. 5 the ship sailed along the ice edge (see Fig. 1), where ice floes less than 1.5-m-thick were dominant in open pack ice. The PDF in Fig. 6b
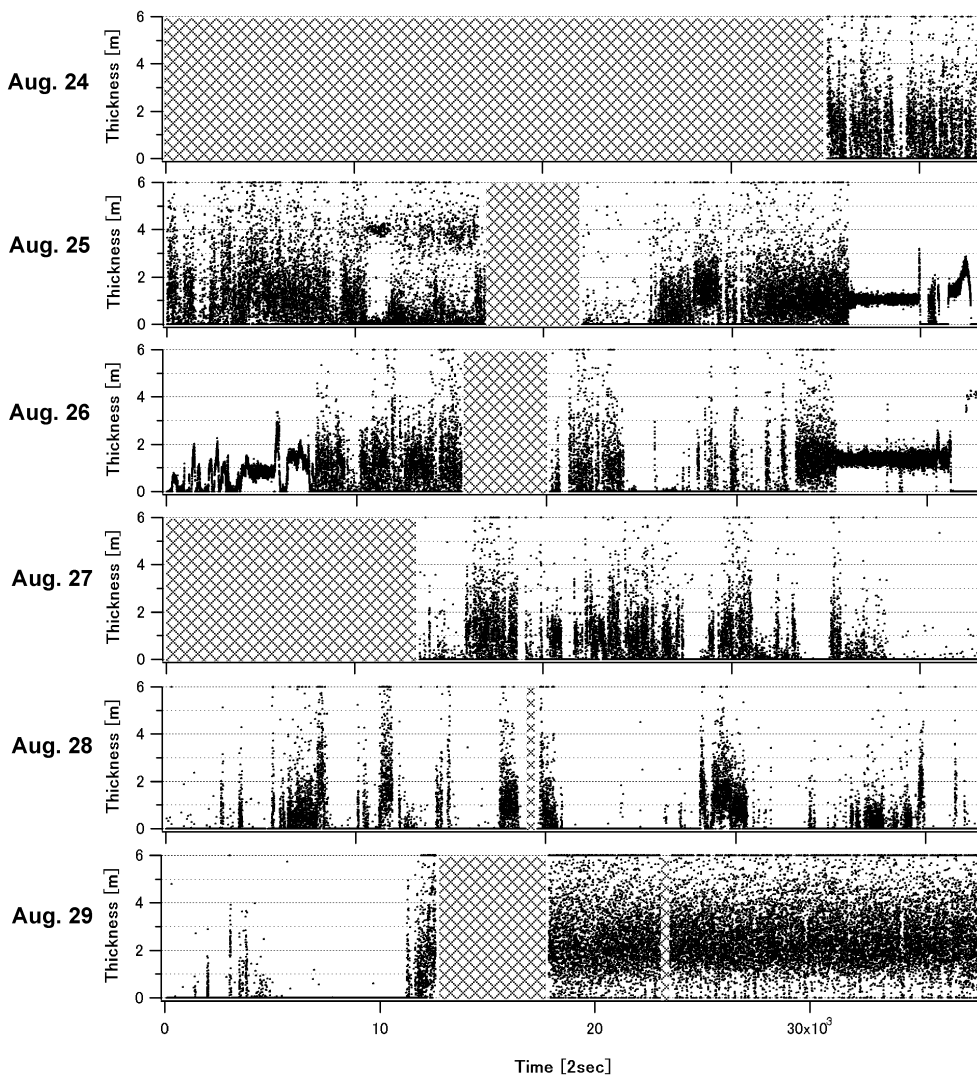

Fig. 4. Time series of total ice thickness by SEM measurements from 24 to 29 August 2003. The x-axis shows time from 0 (00h00m00s) to 43199 (23h59m58s). The hatched area shows no data.
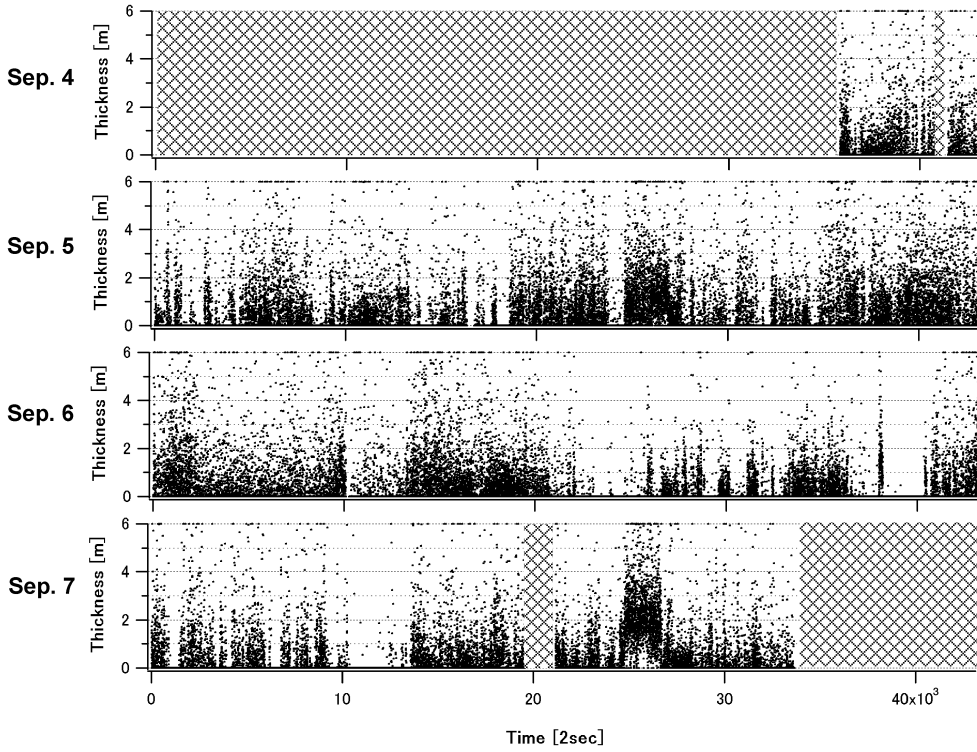
Fig. 5. Time series of total ice thickness by SEM measurement from 4 to 7 September 2003. The x-axis shows time from 0 (00h00m00s) to 43199 (23h59m58s). The hatched area shows no data.
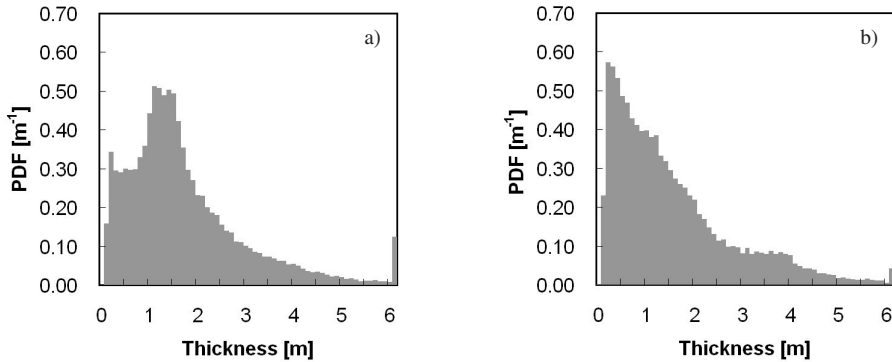

Fig. 6. The probability density function (PDF) in $[m^{-1}]$ of total ice thickness by SEM measurement (a) from 24 to 29 August, and (b) from 4 to 7 September 2003. The bin size is 0.1 m. All ice over 6.1-m-thick was classified as 6.1-m-thick ice.

shows three peaks at around 0.3 m, 1.3 m, and 3 to 4 m thickness, apparently corresponding to level ice, deformed or second-year ice, and multi-year ice, respectively. Although 3 to 4-m-thick multi-year ice floes were observed at around 80°N, they do not appear to be significant in the PDF.

4. Concluding remarks

Measurements of the ice thickness were carried out using a ship-borne electromagnetic induction instrument (SEM) mounted on the R/V *Xuelong* during the Second Chinese National Arctic Research Expedition (CHINARE-2003). SEM observations were conducted during the period from 19 August to 9 September 2003 in the Chukchi Sea. The SEM data were reduced to a 1-D multi-layer model, consisting of the three layers snow, ice and sea-water.

The time series of total (snow plus sea ice) thickness obtained during SEM observations indicate that deformed and second-/multi-year ice floes appeared frequently in very close pack ice farther from the ice edge, while thinner ice floes less than 1.5 m were frequently found in open pack ice along the ice edge. The PDFs show that peaks appear at around 0.3 m, 1.3 to 1.5 m and 3 to 4 m thickness, presumably corresponding to level ice, deformed or second-year ice, and multi-year ice, respectively.

Acknowledgments

References

Bobylev, L.P., Kondratyev, K.Y., and Johannessen, O.M. (2003): Arctic Environment Variability in the Context of Global Change. Chichester, Praxis Publ., 471 p.

Haas, C. (1998): Evaluation of ship-based electromagnetic-inductive thickness measurements of summer sea-ice in the Bellingshausen and Amundsen Seas, Antarctica. Cold Reg. Sci. Technol., **27**, 1–16.

Haas, C., Gerland, S., Eicken, H. and Miller, H. (1997): Comparison of sea-ice thickness measurements under summer and winter conditions in the Arctic using a small electromagnetic induction device. Geophysics, **62**, 749–757.

Kovacs, A. and Morey, R.M. (1991): Evaluation of portable electromagnetic induction instrument for measuring sea ice thickness. CRREL Rep., **91–12**, 17 p.

McNeill, J.D. (1980): Electromagnetic terrain conductivity measurements at low induction numbers. Geonics Limited Technical Note, **TN-6**, 15 p.

Pfaffling, A., Haas, C. and Reid, J.E. (2004): Empirical processing of HEM data for sea ice thickness mapping. Expanded abstracts, 10th European Meeting of Environmental and Engineering Geophysics, Utrecht, The Netherlands.

Reid, J.E. and Vrbancich, J. (2004): A comparison of the inductive-limit footprints of airborne electromagnetic systems. Geophysics, **69**, 1229–1239.

Reid, J.E., Worby, A.P., Vrbancich, J. and Munro, A.I.S. (2003): Ship-borne electromagnetic measurement of Antarctic sea-ice thickness. Geophysics, **68**, 1537–1546.

Tateyama, K., Shirasawa, K., Uto, S., Kawamura, T., Toyota, T. and Enomoto, H. (2006): Standardization of electromagnetic-induction measurements of sea-ice thickness in polar and sub-polar seas. Ann. Glaciol. (in press).

Uto, S., Shimoda, H. and Izumiyama, K. (2002): Ship-based sea ice observations in Lützow-Holm Bay, East Antarctica. Proc 16th IAHR Symp., Dunedin, New Zealand, 218–224.

Worby, A.P., Lytle, V.I. and Massom, R.A. (1999): On the use of electromagnetic induction sounding to determine winter and spring sea ice thickness in the Antarctic. Cold Reg. Sci. Technol., **29**, 49–58.